PCCP

# Investigation of metastable structures of polyiodide in acetonitrile studied by the global reaction route mapping and reference interaction site model self-consistent field explicitly including constrained spatial electron density distribution



| | |
|---|---|
| Journal: | *Physical Chemistry Chemical Physics* |
| Manuscript ID | CP-COM-06-2022-002719.R1 |
| Article Type: | Paper |
| Date Submitted by the Author: | 31-Aug-2022 |
| Complete List of Authors: | Suda, Kayo; The University of Tokyo<br>Yokogawa, Daisuke; The University of Tokyo, |
| | |

ARTICLE

# Investigation of metastable structures of polyiodide in acetonitrile studied by the global reaction route mapping and reference interaction site model self-consistent field explicitly including constrained spatial electron density distribution

Received 00th January 20xx,
Accepted 00th January 20xx

DOI: 10.1039/x0xx00000x

Kayo Suda,*[a] Daisuke Yokogawa*[a]

In this study, we theoretically analyzed metastable structures of polyiodide ($I_7^-$) in gas and acetonitrile phases using the grobal reaction route mapping and the reference interaction site model self-consistent filed explicity including constrained spatial electron density distribution. Considered from chemical reaction pathways of $I_7^-$ in acetonitrile, it was found that there would be 2 types of isomerization pathways. One proceeds with the constant stoichiometry, and another take place by breaking and formation of I-I bonds. In addition, we discovered that $I_7^-$ had various metastable structures within ~10 kcal/mol. Compared the most stable structure in gas and acetonitrile phases, tetrapot type is the most stable strucure in gas phase, however, that one is zigzag type in acetonitrile. In order to clarify this difference, we performed decomposition alalysis of the thermal correlation term in gas and acetonitrile phases. It was found that thermal correction plays a key role in the stability and we could explain the difference of population of EQ states of $I_7^-$ in each phase. Comprehensively, we revealed that the solvation effect must be one of crutial factors to stabilize the isomers of $I_7^-$ and to determine the chemical reaction pathways.

## 1. Introduction

Polyiodides are structurally varied and very complicated compounds.[1, 2] Furthermore, polyiodide properties have been used in various applications, including dye-sensitized solar cells,[3] metal–organic frameworks (MOFs),[4] and single wall[5] and multiwalled carbon nanotubes.[6] Because of their unique physicochemical properties,[1] polyiodides are useful compounds and have been studied with some experimental methods.[7-12] However, most of them are related to kinetic studies and their structures in solution phase are still being investigated.

In the case of $I_3^-$, quantum chemical approaches with solvation effect had been applied,[13-15] and bonding characters and structures have been studied in detail. On the other hand, the number of studies about larger polyiodide, such as $I_7^-$, in solutions is still limited. According to a previous study,[16] the optimized structure of $I_7^-$ (tetrapot type) in the gas phase and acetonitrile had been investigated using experimental and theoretical approaches. In another previous study,[1] the equilibrium structures of $I_7^-$ were reported to be tetrapot and zigzag types. Nevertheless, due to the hypervalent character of the iodide atom,[1] other metastable structures should be present in the solution. Thus, we used theoretical calculations to investigate metastable structures and their $I_7^-$ population in acetonitrile.

Most of the structure searches in quantum chemical computations have been conducted based on the researchers' knowledge. This method usually works well for organic compounds. However, in the case of polyiodide, the number of covalent bonds significantly depends on the surrounding environment, making it difficult to image the number of bonds intuitively. In this study, we applied global reaction route mapping (GRRM) to tackle this difficulty. GRRM has been developed and systematic prediction of unknown, unexpected chemical reaction pathways is possible.[17, 18] Thus, we considered that GRRM must be a suitable approach to investigate unknown metastable structures of $I_7^-$ in acetonitrile. Besides the quantum calculations using GRRM, we applied the solvation theory to examine the effect of solvation on the structure. We selected a reference interaction site model self-consistent field that explicitly included constrained spatial electron density distribution (RISM-SCF-cSED), which is one of the hybrid approaches between quantum and statistical mechanics, as described in our previous studies.[19-26] Because of the small computational cost of RISM-SCF-cSED, we can not only couple the RISM-SCF-cSED with GRRM, but also evaluate the solvation effect using sophisticated quantum chemical approaches, such as coupled cluster methods. This study investigates the counterintuitive metastable structures of $I_7^-$ in acetonitrile and determines its population by applying GRRM and RISM-SCF-cSED.

[a] Graduate School of Arts and Sciences, The University of Tokyo, 3-8-1 Komaba, Meguro-ku, Tokyo 153-8902, Japan.

† Footnotes relating to the title and/or authors should appear here.
Electronic Supplementary Information (ESI) available: [details of any supplementary information available should be included here]. See DOI: 10.1039/x0xx00000x

## 2. Theoretical methods

We performed geometry optimizations in gas and solution phases (acetonitrile) using the B3LYP-D3/ECP-def2-SVPD level of theory with software (GRRM14) and the GAMESS program.[27] The RISM integral equation was coupled with the hypernetted-chain closure. The temperature was 300 K, and the acetonitrile density was 0.0115 molecules Å$^{-3}$. The Lennard–Jones parameters for the solute and solvent molecules were calculated using the OPLS-AA parameter.[28]

First, we determined the equilibrium (EQ) and transition (TS) structures of $I_7^-$ in the gas phase applying GRRM. We performed EQ and TS geometry optimization in acetonitrile using these structures as initial structures. Frequency calculations confirmed the EQ and TS structures in the solution. We calculated the energy of the obtained structures $I_7^-$ in each phase using the coupled-cluster singles and doubles with perturbative triples using aug-cc-pVTZ-PP level of theory. The obtained energy value was summarized as follows:

$$\Delta G = \Delta G^{\mathrm{sol}} + \Delta G^{\mathrm{corr}}, \quad (1)$$

where $\Delta G^{\mathrm{corr}}$ represents the thermal correlation calculated from the frequency calculations and

$$\Delta G^{\mathrm{sol}} = \langle \psi^{\mathrm{sol}} | \hat{\mathcal{H}} | \psi^{\mathrm{sol}} \rangle + \Delta\mu, \quad (2)$$

where $\Psi^{\mathrm{sol}}$ represents a wavefunction determined in solution and $\Delta\mu$ represents the solvation free energy calculated by RISM-SCF-cSED. Based on this result, we also calculated the population of the obtained structures of $I_7^-$ in each phase.

## 3. Results and discussion

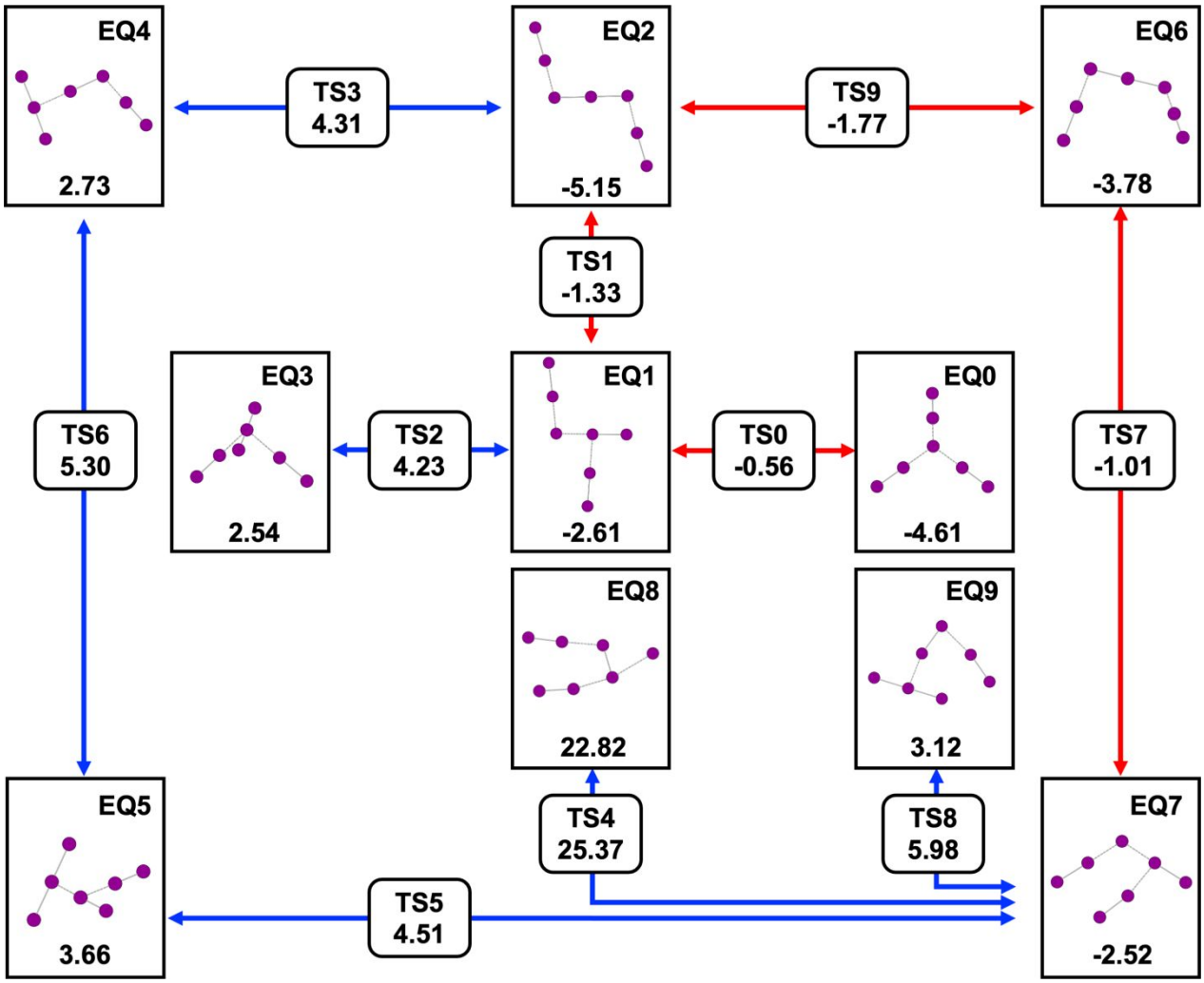


**Scheme 1. Chemical reaction pathways of $I_7^-$ in acetonitrile. The origin of the energy was $\Delta G(I_3^-) + 2\Delta G(I_2)$ in acetonitrile and relative energies were shown in kcal/mol.**

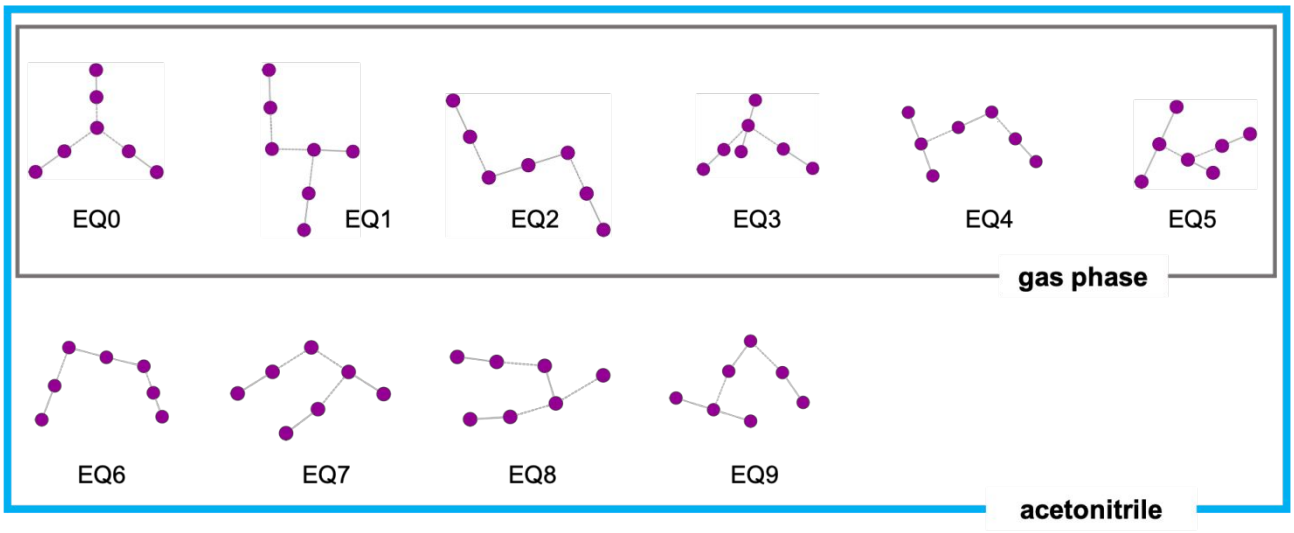


of $I_7^-$ in gas phase and acetonitrile.

$$I_3^- + 2I_2 \leftrightarrows I_7^-,$$

**Table 1. Free energy differences of $I_7^-$ of each structure in each phase (unit: kcal/mol).**

| | Gas phase | Acetonitrile |
|---|---|---|
| EQ0 | 0.00[a] | 0.54 |
| EQ1 | 3.43 | 2.54 |
| EQ2 | 0.95 | 0.00[b] |
| EQ3 | 8.62 | 7.69 |
| EQ4 | 9.24 | 7.88 |
| EQ5 | 10.40 | 8.81 |
| EQ6 | – | 1.37 |
| EQ7 | – | 2.63 |
| EQ8 | – | 27.97 |
| EQ9 | – | 8.27 |

a: Free energy is −2064.06467 hartree.

b: Free energy is −2064.09343 hartree.

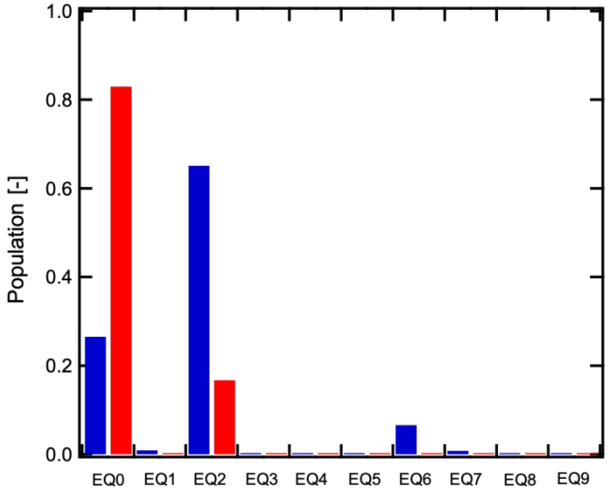


**Fig. 1 Populations of isomers of $I_7^-$ in gas (red) and acetonitrile (blue) phases.**

Scheme 1 shows the chemical reaction pathways of $I_7^-$ in acetonitrile. We obtained 10 equilibrium structures (EQ0-9) and 10 transition structures (TS0-9) of $I_7^-$ in acetonitrile. In the case of polyiodide, $I_3^-$ is well known to be stable in solution. Therefore, in this study, we also considered the following decomposition process:

and the origin of the free energies in Scheme 1 was set to be $\Delta G(I_3^-) + 2\Delta G(I_2)$. When the energy of the state is negative, the state is more stable than $I_3^- + 2I_2$, while $I_3^- + 2I_2$ is stable when the energy is positive. Based on the sign of the energies in Scheme 1, we can discuss the possibility of the decomposition from $I_7^-$ to $I_3^-$. Focused on the chemical reaction pathway (shown by red arrow), we found that the chemical reaction pathway (from EQ0 to EQ7 through EQ1, EQ2 and EQ6) could be occurred with the same stoichiometry because relative energies of TS and EQ states had negative value. On the other hand, relative energies of TSs of another chemical reaction pathway (shown by blue arrow) had positive value. This means that structural change of $I_7^-$ could be occurred through the decomposition of $I_7^-$ to $I_3^-$ and $2I_2$. In the previous studies,[1, 29] it was found that the structural change of $I_7^-$ in solid phase could be occurred through the decomposition of $I_7^-$ to $I_3^-$ and $2I_2$ because $I_3^-$ and $I_2$ are stable structures. These experimental observations suggest that our findings could provide us with reliable information. In next section, we focused on the obtained equilibrium structures of $I_7^-$ and its features in gas and acetonitrile phases.

Scheme 2 shows the obtained equilibrium structures of $I_7^-$ in the gas phase (EQ0–EQ5) and acetonitrile (EQ0–EQ9). $I_7^-$ could take various conformations such as tetrapot and zigzag types due to the hypervalent character of iodide atom. With this result, we can say that GRRM could be a useful tool for investigating systems, which have various conformations since

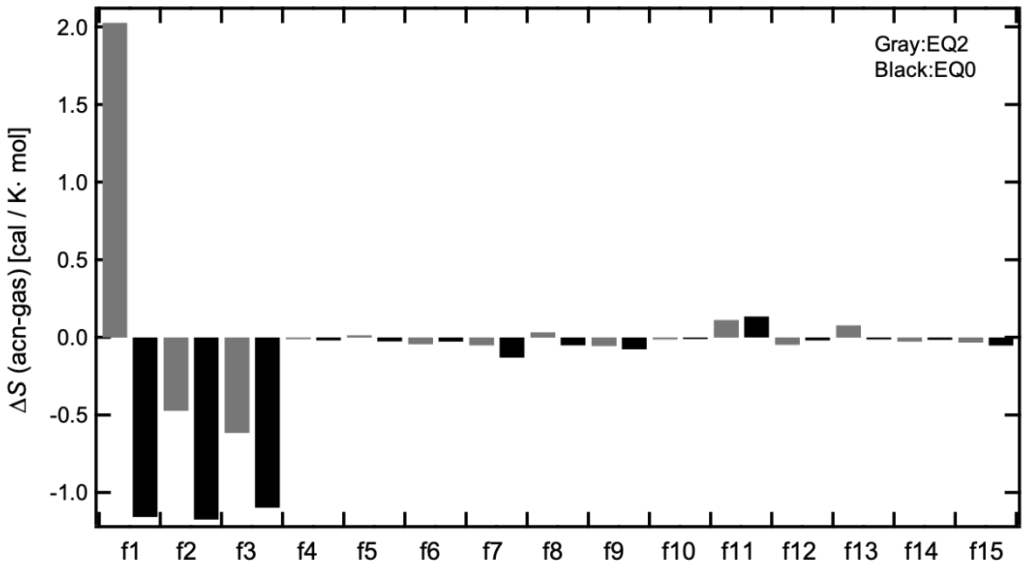


**Fig. 2 Entropy difference (Δ*S*) of EQ0 and EQ2 between acetonitrile and gas phases (unit: cal / K·mol).**

it would be difficult for us to analyze by hand. Although there were small differences between the structures obtained in acetonitrile and gas phases, it was discovered that the structures of EQ0–EQ5 in acetonitrile were similar to those in the gas phase. Focused on some structures in each phase, tetrapot type (EQ0) and zigzag type (EQ2) were obtained in each phase, which was described in previous studies,[1, 16, 29] so that our findings could provide us with reliable information. In the cases of EQ6, EQ7, EQ8, and EQ9 in acetonitrile, these structures were obtained from transition state structures in the gas phase, indicating that the structures of $I_7^-$ would be influenced by the solvation effect. The details of the obtained structures in each phase were described in the Supporting Information.

Next, we calculated the energies in the gas and acetonitrile phases. Table 1 demonstrates the free energy differences ($\Delta\Delta G$) from the most stable structure in each phase. Although there are considerable differences in the geometry, we discovered that the obtained energies in each phase were within ~10 kcal/mol except for EQ8. In the case of the gas phase, EQ0 was the most stable structure, whereas EQ2 was the most stable structure in the case of acetonitrile. Since the zigzag type structure was reported in MOF,[4] the surrounding environment, such as solvent and MOF, should be a crucial factor in stabilizing the zigzag type structure.

There should be some isomers in the gas and acetonitrile phases due to the small energy differences. As shown in Fig. 1, we calculated the population of each isomer in each phase using the data of free energy differences. EQ0 and EQ2 were the dominant isomers in each phase. Furthermore, the population trends of EQ0 and EQ2 in the gas phase were inverted compared with acetonitrile. In the case of the gas phase, the population of isomers except for EQ0 and EQ2 were negligible. However, isomers of EQ0, EQ1, EQ2 and EQ6 existed in the case of acetonitrile. This result would be consistent with the chemical reaction pathways of $I_7^-$ in acetonitrile as described in Scheme

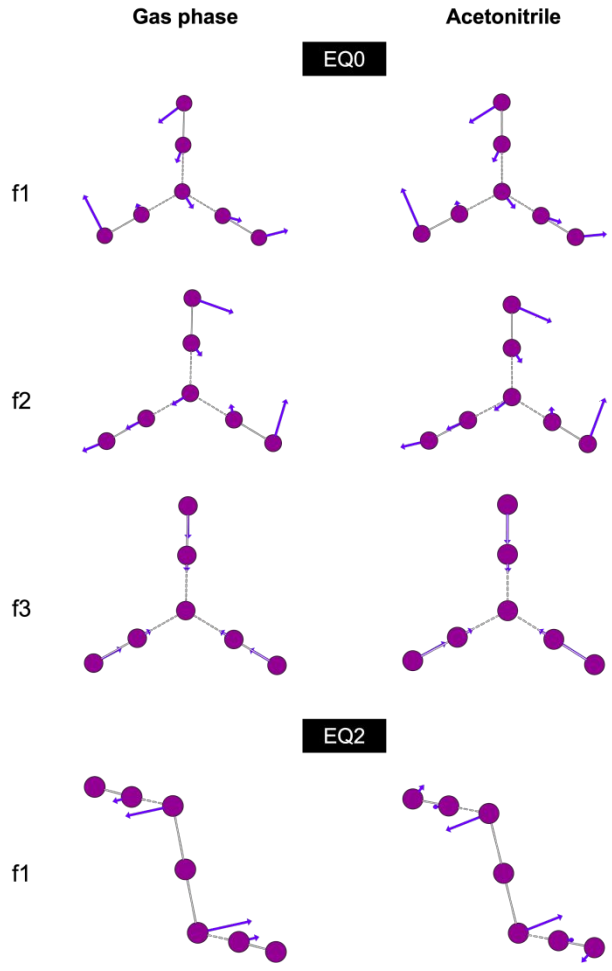


**Fig. 3 Normal modes with low frequencies in gas and acetonitrile phases (Purple arrows represent directions of the motion of each atom).**

1. In the previous studies,[4, 16] the presence of $I_7^-$ in solutions was reported. However, the population of each isomer was not clarified to our knowledge. Based on these findings, it was discovered that polyiodides in solution must be considered with the solvation effect.

Why does the most stable isomer change from EQ0 to EQ2 in acetonitrile? To answer the question, we divided $\Delta G$ into $\Delta G^{\mathrm{sol}}$ and $\Delta G^{\mathrm{corr}}$. As shown in the Supporting Information, when $\Delta G^{\mathrm{corr}}$ is omitted, EQ0 becomes the most stable in both phases, indicating that $\Delta G^{\mathrm{corr}}$ determines the relative stabilities between EQ0 and EQ2. To discuss the difference in the stability in more detail, the decomposition analysis of $\Delta G^{\mathrm{corr}}$ would be helpful. $\Delta G^{\mathrm{corr}}$ can be divided into the three terms: translation, rotation, and vibration terms. In the case of $I_7^-$ in acetonitrile, we discovered that the $\Delta G^{\mathrm{corr}}$ that comes from vibrational modes played a critical role in the stability among the isomers. Fig. 2 shows that entropy differences in the vibrational modes of EQ0 and EQ2 between acetonitrile and gas phases. In the case of EQ0, the lowest frequency (f1), second lowest frequency (f2) and third lowest frequency (f3) had negatively large values. This means that EQ0 in gas phase would be more flexible than that in acetonitrile. This is the reason why EQ0 would be more unstable in acetonitrile phase than that in gas phase. On the other hand, f1 had a positively large value in the case of EQ2. This means that the EQ2 would be more flexible in acetonitrile than that in gas phase, which leads to the stability of the EQ2 in acetonitrile. Because EQ0 is destabilized and EQ2 is stabilized in acetonitrile, the most stable isomer changes from EQ0 to EQ2 in acetonitrile.

Before we close this section, it is better to discuss the character of the normal modes (f1, f2 and f3 of EQ0 and f1 of EQ2) in gas and acetonitrile phases. In Fig. 3, these normal modes in each phase were summarized. In the case of EQ0, f1 and f2 are the vending modes, and f3 is the stretching mode. f1 of EQ2 is the distortion mode. Because the directions of each motion do not change drastically with the solvation effect, the solvation effect should affect the force constant of these normal modes. The reason why the solvation effect changed the force constant will be discussed in the future work.

## 4. Conclusions

In this study, we theoretically analyzed metastable structures of $I_7^-$ in acetonitrile employing GRRM and RISM-SCF-cSED. Some isomers and transition states were discovered in acetonitrile, and they were affected by the solvation effect. Considered from chemical reaction pathways, there would be 2 types of isomerization pathways. One proceeds with the constant stoichiometry, and another take place by breaking and formation of I-I bonds. Focused on EQ structures, it was found that the most stable EQ structure is tetrapot type (EQ0) in gas phase, meanwhile, zigzag type (EQ2) is the most stable structure in acetonitrile. In order to clarify the difference, we tried to perform the decomposition analysis of thermal correlation terms on EQ0 and EQ2 in gas and acetonitrile phases. It was found that thermal correlation determined by frequency computations is a critical factor to determine the stability of $I_7^-$ in acetonitrile.

In this study, the structures in acetonitrile were determined from the structures determined in gas phase using GRRM. However, for the complicated systems, it is strongly required that GRRM should be coupled with RISM-SCF-cSED and the structures in solution should be obtained automatically. This is our feature study.

## Conflicts of interest

There are no conflicts to declare.

## Acknowledgements

This work is supported in part by a grant from the Institute for Quantum Chemical Exploration (IQCE). D. Y. is thankful for the support from JSPS KAKENHI Grant Number JP19K05367, JST, PRESTO Grant Number JPMJPR21C9, and the Leading Initiative for Excellent Young Researchers. The authors would like to thank Enago (www.enago.jp) for the English language review.

## Notes and references

1. P. H. Svensson and L. Kloo, *Chem. Rev.*, 2003, **103**, 1649-1684.
2. K. Sonnenberg, L. Mann, F. A. Redeker, B. Schmidt and S. Riedel, *Angew. Chem. Int. Ed.*, 2020, **59**, 5464-5493.
3. B. Li, L. Wang, B. Kang, P. Wang and Y. Qiu, *Sol. Energy Mater. Sol. Cells*, 2006, **90**, 549-573.
4. Z. Yin, Q.-X. Wang and M.-H. Zeng, *J. Am. Chem. Soc.*, 2012, **134**, 4857-4863.
5. M. Chorro, G. Kané, L. Alvarez, J. Cambedouzou, E. Paineau, A. Rossberg, M. Kociak, R. Aznar, S. Pascarelli, P. Launois and J. L. Bantignies, *Carbon*, 2013, **52**, 100-108.
6. E. Ramasamy, W. J. Lee, D. Y. Lee and J. S. Song, *Electrochem. Commun.*, 2008, **10**, 1087-1089.
7. R. S. Mulliken, *J. Am. Chem. Soc.*, 1952, **74**, 811-824.
8. O. E. Myers, *J. Chem. Phys.*, 1958, **28**, 1027-1029.
9. R. W. Ramette and R. W. Sandford, *J. Am. Chem. Soc.*, 1965, **87**, 5001-5005.
10. E. E. Genser and R. E. Connick, *J. Chem. Phys.*, 1973, **58**, 990-996.
11. T. Sano, H. Hori, M. Yamamoto and T. Yasunaga, *Bull. Chem. Soc. Jpn.*, 1984, **57**, 575-576.
12. V. T. Calabrese and A. Khan, *J. Phys. Chem. A*, 2000, **104**, 1287-1292.
13. H. Sato, F. Hirata and A. B. Myers, *J. Phys. Chem. A*, 1998, **102**, 2065-2071.
14. T. Koslowski and P. Vöhringer, *Chem. Phys. Lett.*, 2001, **342**, 141-147.
15. C. J. Margulis, D. F. Coker and R. M. Lynden-Bell, *Chem. Phys. Lett.*, 2001, **341**, 557-560.
16. M. Groessl, Z. Fei, P. J. Dyson, S. A. Katsyuba, K. L. Vikse and J. S. McIndoe, *Inorg. Chem.*, 2011, **50**, 9728-9733.

17. S. Maeda, K. Ohno and K. Morokuma, *Phys. Chem. Chem. Phys.*, 2013, **15**, 3683-3701.
18. K. Ohno, *Chemical Record*, 2016, **16**, 2198-2218.
19. D. Chandler and H. C. Andersen, *J. Chem. Phys.*, 1972, **57**, 1930-1937.
20. F. Hirata and P. J. Rossky, *Chem. Phys. Lett.*, 1981, **83**, 329-334.
21. S. Ten-no, F. Hirata and S. Kato, *Chem. Phys. Lett.*, 1993, **214**, 391-396.
22. H. Sato, F. Hirata and S. Kato, *J. Chem. Phys.*, 1996, **105**, 1546-1551.
23. D. Yokogawa, H. Sato and S. Sakaki, *J. Chem. Phys.*, 2007, **126**.
24. D. Yokogawa, *Chem. Phys. Lett.*, 2013, **587**, 113-117.
25. D. Yokogawa, *Bull. Chem. Soc. Jpn.*, 2018, **91**, 1540-1545.
26. D. Yokogawa and K. Suda, *J. Chem. Phys.*, 2021, **155**, 204102.
27. M. W. Schmidt, K. K. Baldridge, J. A. Boatz, S. T. Elbert, M. S. Gordon, J. H. Jensen, S. Koseki, N. Matsunaga, K. A. Nguyen, S. J. Su, T. L. Windus, M. Dupuis and J. A. Montgomery, *J. Comput. Chem.*, 1993, **14**, 1347-1363.
28. W. L. Jorgensen, D. S. Maxwell and J. TiradoRives, *J. Am. Chem. Soc.*, 1996, **118**, 11225-11236.
29. R. Poli, J. C. Gordon, R. K. Khanna and P. E. Fanwick, *Inorg. Chem.*, 1992, **31**, 3165-3167.